ISSN 0027-1349, Moscow University Physics Bulletin, 2015, Vol. 70, No. 5, pp. 390–396. © Allerton Press, Inc., 2015.
Original Russian Text © D.A. Popov, A.B. Vasiliev, V.G. Voronin, O.E. Nanii, V.N. Treshchikov, 2015, published in Vestnik Moskovskogo Universiteta. Fizika, 2015, No. 5, pp. 61–67.

## OPTICS AND SPECTROSCOPY. LASER PHYSICS

# Multichannel Fiber Lasers Anchored on the ITU Grid

**D. A. Popov[a,b], A. B. Vasiliev[a], V. G. Voronin[a], O. E. Nanii[a,b], and V. N. Treshchikov[b]**

[a] *Department of Physics, Moscow State University, Moscow, 119991 Russia*
[b] *T8 LLC, ul. Krasnobogatyrskaya 44/1, office 826, Moscow, 107076 Russia*
*e-mail: popov.demid@gmail.com, naniy@t8.ru*
Received April 3, 2015; in final form, June 8, 2015

**Abstract**—We propose a multichannel erbium-doped-fiber ring laser in which the spatial separation of 40 spectral channels is produced by a pair of dispersive elements: a multiplexer and demutliplexer. Both 2- and 3-channel generation modes with the possibility of channel switching and power control were used and studied experimentally. The long-term stability of these generation modes on a several-hour time scale is at least 10%. The generation characteristics are described satisfactorily by a simple phenomenological model. In the framework of this model the interaction between the generation channels, which stems from saturation in the active media, is determined by the cross-saturation coefficients, which depend on the frequency spacing between the channels. Good agreement was found between the experimentally measured spectral dependence of the cross saturation and the spectral shape of the holes in the gain spectrum of the erbium amplifiers. In the three-channel generation mode, suppression of the central channel occurs with an increase in the pumping power. An explanation of this effect is given.

*Keywords*: multi-frequency laser, multichannel laser, ring laser, erbium-doped-fiber laser, wavelength multiplexing, multichannel telecommunication system, telecommunication frequency grid.

**DOI:** 10.3103/S0027134915050124

## INTRODUCTION

The interest in lasers that are capable of generation at several wavelengths stems from the possibilities for their application in different areas of science and technology. Multichannel lasers have advantages in comparison with single-mode lasers in such application areas as interferometry, laser distance ranging, holography, environmental monitoring, and differential measurement methods. They may be used to design high sensitivity and precision devices and instruments [1–6]. Multichannel laser applications in radiophotonics are a new trend [7]. Another area is optical fiber communications, where multichannel lasers may be used for testing multichannel communications systems with spectral multiplexing (DWDM) [8–15].

Gas-phase lasers were the first multichannel lasers. Because of the non-homogeneous broadening of the active media, it is rather straightforward to obtain stable multichannel generation using these lasers [2, 5]. Replacement of the gaseous active media with a solid-state active media at the next step led to a significant increase in the durability, reliability, efficiency, and manufacturability of multichannel lasers [16–19].

Several methods to decrease the competitive interaction between the generation channels that arise due to the homogeneous broadening of the amplification band in solid-state lasers have been suggested and investigated. The most general leveling method for the power of generation channels is the automatic adjustment of the losses in the individual channels. With the use of this method, highly stable bidirectional generation modes in solid-state ring lasers have been obtained [3, 20]. Other methods that have been proposed to decrease mode competition are spatial and polarization frequency spacings of generation channels in active media [18, 19, 21–25] and non-linear optical methods for stabilizing the multichannel generation [26–28].

Testing modern high-speed optical-fiber communication systems with spectral multiplexing (DWDM communication systems) requires a multichannel light source that is tunable in the 1530–1560 nm region [8–14]. The most promising source of this type is the erbium-doped-fiber laser (EDFL). The multichannel generation mode for this laser has been studied in a number of works [1, 29–32].

As was shown in [1], stable two-channel generation with desired generation wavelengths may be obtained by careful adjustment of losses in generation channels. However, this laser design was not able to provide wavelength tunability in the entire C-region and provide multichannel generation with more than two channels.

In this work, we used a telecommunication spectral multiplexer–demultiplexer as a narrow band filter; these are applied in optical-fiber communication lines

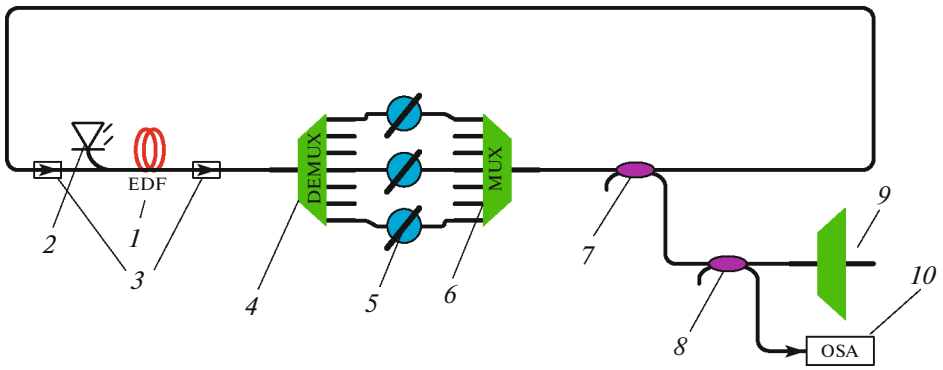


**Fig. 1.** The experimental device: an erbium-doped fiber (*1*), a diode pump laser (*2*), an optical insulator (*3*), multiplexers (*4*, *6*, *9*), a tunable attenuator (*5*), optical splitters (*7*, *8*), and an optical spectrum analyzer (*10*).

to obtain the standard spectral frequency grid [11–15] with a step of 100 GH. Our laser design allowed us to test the feasibility of multichannel generation with numbers of channels from 2 to 40. We studied the two- and three-channel generation modes in detail and demonstrated that it is possible to tune each channel in the entire C-region (1530–1560 nm). In the three-channel generation mode, we observed and explained the effect of central channel suppression with an increase in pumping power.

## 1. THE EXPERIMENTAL DEVICE

Figure 1 shows the scheme of the proposed multichannel laser. A standard erbium-fiber amplifier of the type that is applied in optical communication systems was used as the amplifying media. The active element, an erbium-doped fiber (*1*), is pumped by a diode laser (*2*) that emits at 980 nm. The pump current is varied in the 60–300 mA region. One-directional generation was obtained using built-in optical isolators (*3*) at the amplifier input and output, which protect the amplifier against reflected emissions. The OM-40-AV-PM 40-channel multiplexer-demultiplexer (*4*) at the amplifier output divides the radiation into 40 channels. The spectral frequency spacing between the channel is 100 GHz. The outputs of the work channels are coupled with the inputs of tunable attenuators (*5*). In turn, the attenuator outputs are coupled with the inputs of the corresponding channels of a second multiplexer (*6*). The emission that is combined in the second multiplexer is directed to the input of the amplifier. For each channel, the attenuation is individually controlled using programmable attenuators (*5*). The range of dynamic tuneability of the VOA attenuators is 0.1–30 dB. The multiplexer–demultiplexer pair provides spatial frequency spacing and then merging of up to 40 spectral channels. Part of the radiation is taken out of the resonator via a 10% splitter (*7*). Using a 1% splitter (*8*) the 1% beam is directed to a spectral analyzer (*9*) (Anritsu MS9710B) and the 99% beam is directed to an Im-40-AV-PM multiplexer (*10*), which is used for the coarse measurement of power in each channel during the initial adjustment. The MS9710B Anritsu spectral analyzer is capable of recording radiation in the 600–1750 nm region with a power in the region from –90 to +10 dB. The wavelength measurement uncertainty is +50 pm.

The two-channel generation mode was studied using either the general scheme of the multichannel laser (Fig. 1) or a simplified scheme in which the OM-40-AV-PM demultiplexer (*6*) was replaced by a 50% splitter. The results that are presented in the next section were obtained for both of these schemes.

## 2. A STUDY OF TWO-CHANNEL GENERATION

In the course of this work stable generation was demonstrated for arbitrary channel pairs from the nearest C38 (1546.92 nm) to C40(1545.32 nm) (0.80 nm) to the most remote C21 (1560.61 nm) to C40 (1545.32 nm) (15.29 nm) at a pump current above 250 mA. At a current of 200 mA the powers of the C21 and C40 channels after adjustment by the VOA attenuator are –15.78 and –15.09 dB, respectively. A decrease in the pump current to a value below 200 mA results in significant changes in the ratio of the channel powers.

The non-monotonic dependences of the channel powers on the pump current can be explained by changes in the polarization-dependent losses as the pump current varies. The experimental measurements showed that the sensitivity to a change in the losses in one channel is significantly larger than that to a change in the losses simultaneously in two channels. The sensitivity to the change in the losses in one channel increases as the spectral spacing between the channels decreases and, vice versa, decreases as the frequency spacing increases. In the experiment, the channel losses were tuned by varying the VOA transmission coefficient. Figure 2 shows the dependences of the channel powers on the transmission coefficient of the controlled channel. The obtained plots have the

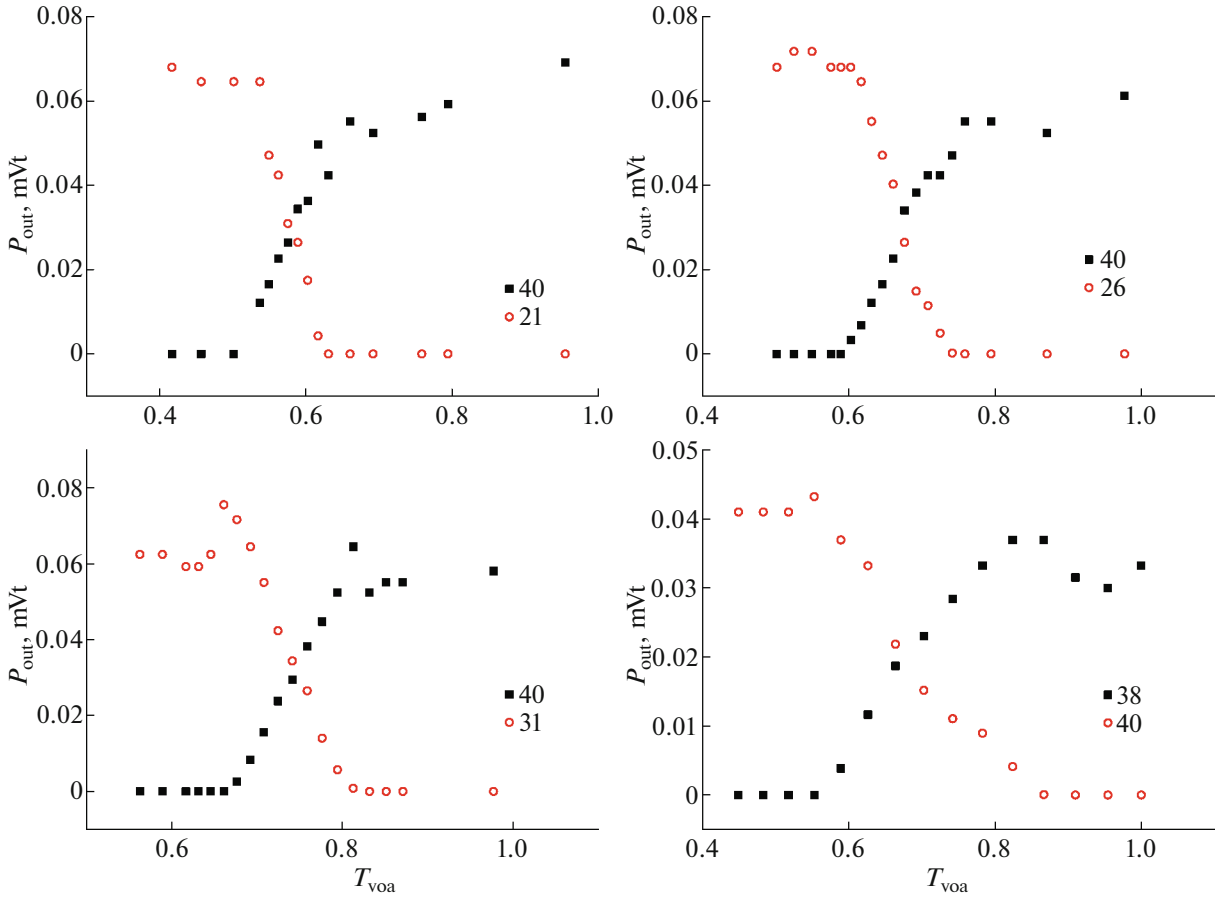


**Fig. 2.** The dependences of the powers of the channels on the losses in the controlled channel (black squares). $T_{voa}$ is the attenuator transmission coefficient. The channel numbers are given in the legends.

characteristics of the two-channel generation X-shaped form.

The temporal stability of the two-channel generation for different pairs of channels was studied at a pumping current of 300 mA. The temporal instability of two channels with a large spectral frequency spacing (C21 and C40) does not exceed 0.6%, while for a pair of closer channels (C36 and C40) it is rather large, viz., it reaches 3%.

Our experimental studies showed that at a pumping current of 300 mA, stable two-channel generation can be obtained for any pair of 40 channels of the standard grid of the telecommunication frequencies in the region from 196.1 THz (1528.77 nm) to 192.20 THz (1559.79 nm). The correspondence between the spectral channel numbers and the frequencies (wavelengths) in the grid of the International Electro-communication Union was given in [36].

## 3. A STUDY OF THREE-CHANNEL GENERATION

Three-channel generation was obtained for any three of the 40 channels. Similar to the two-channel case, the stability of three-channel generation improves as the frequency spacing between the channels increases. Switching of the generation channels in the working laser was demonstrated experimentally. The minimal frequency spacing between the working channels was 100 GHz (generation in the neighboring channels).

Figure 3a shows the spectrum of three-channel generation with the working channels 39 (1559.79 nm), 40 (1560.61 nm), and 41 (1561.42 nm). A decrease in the power of the central channel is observed in this generation mode as the powers of the other two channels increase (Fig. 3b). This result can be explained theoretically by assuming that the cross-saturation coefficients decrease as the frequency spacing between them increases. Our measurements of the cross-saturation coefficients confirmed this explanation (see the next section).

When the frequency spacing between the generation channels is above 400 GHz, the three-channel generation is stable in a wide region of the pumping power; the powers of all three generation channels increase steadily as the pumping power increases.

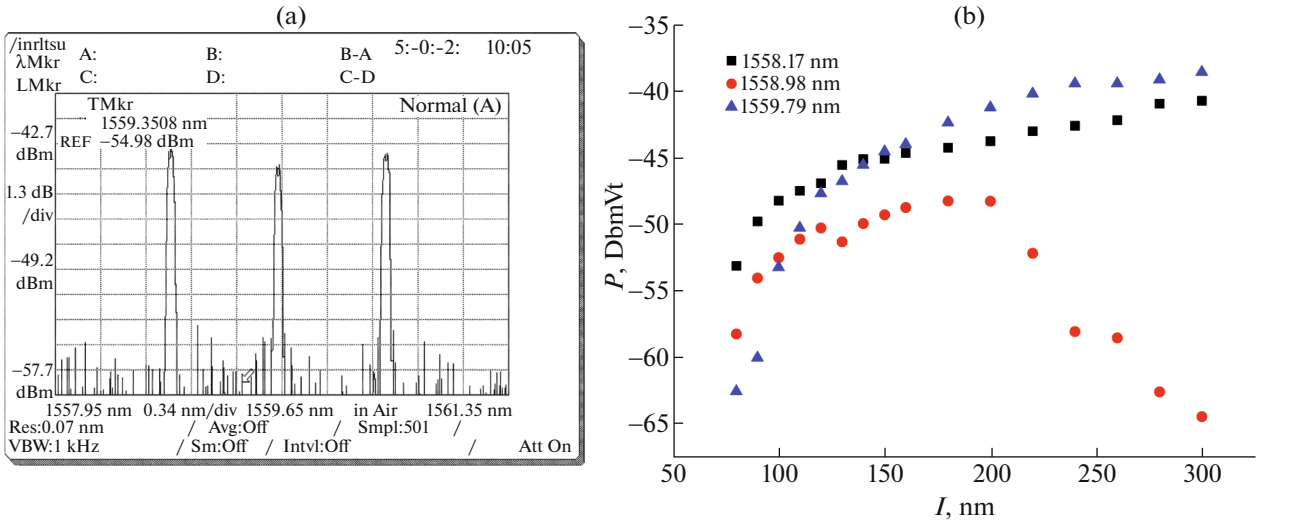


**Fig. 3.** The three-channel generation spectrum at a frequency spacing between the channels of 100 MHz (a) and the dependences of the channel output powers on the pump current (b).

## 4. DISCUSSION OF THE EXPERIMENTAL RESULTS

To describe the multichannel laser we will use the phenomenological equations of the balance approximation taking the inter-channel interaction via saturation of the inverse population into account [33]. The most important parameters that determine the features of the multichannel generation are the cross-saturation coefficients.

The equation system for the normalized powers and gain coefficients has the form

$$\frac{d_i I}{d\tau} = [(h_i - 1 + \delta_i)I_i]G,$$
$$\frac{d_i n}{d\tau} = \alpha_i - n_i(1 + I_i + \sum_{i \neq j} \zeta_i I_j), \quad (1)$$

where $\alpha_i$ is the excess of pumping above the threshold in the corresponding generation channels under the assumption that generation in the neighboring channels is absent, $G = T_1/\tau_{\text{Phot}}$ is the ratio of the inversion population relaxation time to the electric field decay time in the resonator, $I_i$ are the normalized radiation powers in the corresponding channels, $\zeta_{ij}$ are the cross-saturation coefficients, $n_i$ are the normalized amplification coefficients for the corresponding channels, $\delta_i$ are normalized additional losses for the corresponding channels, and $\tau = t/T_1$ is the normalized time.

The two-channel generation is stable only if both cross-saturation coefficients are lower than one. In this case, the output powers of both the channels increase as the pumping power increases. The stationary solutions of system (1) for the case of two channels for which the losses change only in the first channel ($\delta_1 \equiv \delta$, $\delta_2 = 0$) and the cross-saturation coefficients are the same ($\zeta_{12} = \zeta_{12} \equiv \zeta$) have the form [33]

$$I_1 = \frac{\left(\frac{\alpha}{1+\delta} - 1\right) + \zeta(\alpha - 1)}{1 - \zeta^2},$$
$$I_2 = \frac{(\alpha - 1) + \zeta\left(\frac{\alpha}{1+\delta} - 1\right)}{1 - \zeta^2}. \quad (2)$$

As follows from (2), the dependences of the channel powers on the losses in one of them have an X-shaped form in the two-channel generation region. The susceptibility to losses, which is minimal at $\zeta = 0$, grows as $\zeta$ increases, reaching its maximum at $\zeta = 1$. In the latter case the X-shaped dependence transforms to a stepwise dependence, while the width of the two-channel generation region drops to zero. The latter indicates that the switching between the generation channels is due to a change in the value of the losses.

The cross-saturation coefficient $\zeta$ can be determined from the experimental dependences of the channel powers on the losses in one of them. This is done by selecting a value of $\zeta$ for which the best agreement between the theoretical and experimental dependences $I_{1,2}(\delta)$ is attained. As an example, Fig. 4a shows the experimental and theoretical dependences of the powers of two channels on additional losses in the first channel. The theoretical dependences were obtained via numerical solution of Eq. (1) with adjustment of the cross-saturation coefficient. As is seen,

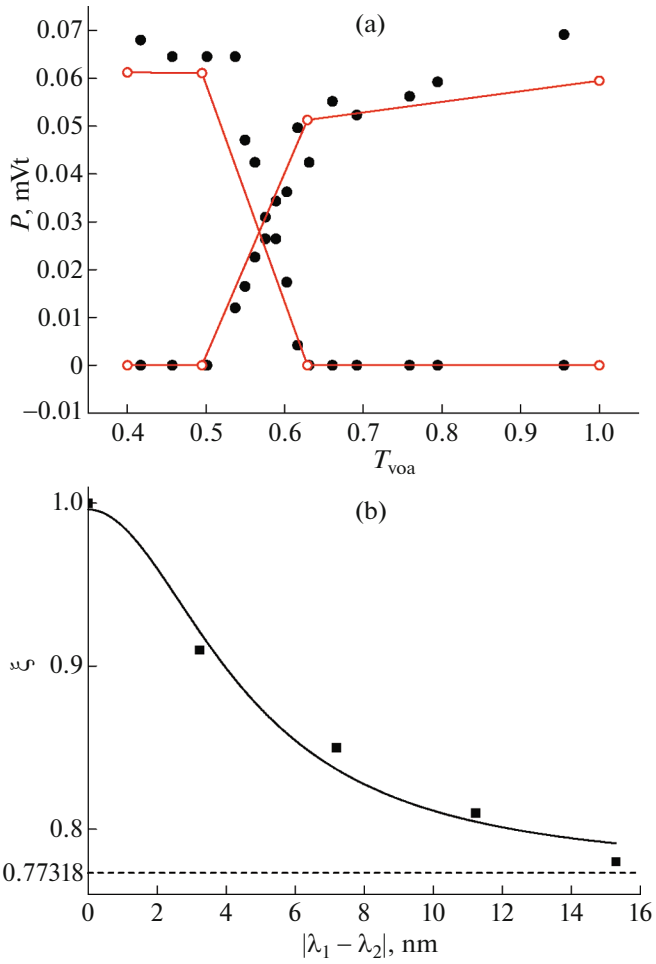


**Fig. 4.** The experimental (dotted curves) and theoretical (solid curves) dependences of the two-channel powers on the attenuator transmission of one of the channels. The match between the experimental and theoretical dependences is provided by the choice of the cross-saturation coefficient value ζ (a). The dependence of the cross-saturation coefficient, ζ, on the frequency spacing between the channels (b).

the experimental and theoretical dependences are in good agreement at ζ = 0.78. The experimental dependences were obtained for channels 21 and 40 at a frequency difference of 1.9 THz.

Using this method we obtained the cross-saturation coefficients for different channel pairs. It turned out that to a first approximation the cross-saturation coefficients, ζ, depend solely on the frequency (wavelength) difference (see Fig. 4b): the cross-saturation coefficient increases as the channel frequencies become closer and, respectively, decreases as the frequency difference increases. The dependence of ζ on the frequency difference can be approximated by a bell-shaped curve (Fig.3b shows half of this curve plotted for the dependence of ζ on the frequency difference module between the channels). The width of the curve coincides with the spectral width of amplification gaps that are measured experimentally [34]. The competition-reducing mechanism in the erbium laser (i.e., the mechanism that is responsible for the fulfillment of the $\zeta < 1$ inequality) is the same as the one that is responsible for the gap in the amplification spectrum of the erbium amplifiers. This question was discussed in [34] and the references cited therein. In our opinion, the gap-formation mechanism is not completely understood as yet and requires further study. Without the gap formation mechanism it appears not to be possible to explain the relatively high stability of the two-channel generation, especially when the frequency difference between the generating channels is above 300 GHz, as was already noted in [35].

As follows from equation system (1) and has been confirmed experimentally, two-channel generation at equal losses and the channel amplification coefficients are stable at any pump power that exceeds the threshold value if the normalized cross-saturation coefficients are less than unity ($\zeta < 1$).

As also follows from equation system (1), three-channel generation is stable at equal losses and channel amplification coefficients, as well if the cross-saturation coefficients for any pair of the channels are less than one ($\zeta_{ij} < 1$) and, in addition, are equal to each other $\zeta_{12} = \zeta_{23} = \zeta_{13}$ However, as follows from Figure 4b, the cross-saturation coefficients of the outermost channels $\zeta_{13}$ are smaller than the cross-saturation coefficients $\zeta_{12}$, $\zeta_{23}$ of the central channel by the outermost channels: $\zeta_{13} < \zeta_{12}, \zeta_{23}$ In this case, if the inequality

$$\zeta_{12} = \zeta_{23} > \frac{1 + \zeta_{13}}{2} \qquad (3)$$

holds, the three-channel generation mode does not occur, because the central channel is suppressed (it is assumed that $\zeta_{12} = \zeta_{23}$ and $\zeta_{ij} = \zeta_{ji}$ for any pair of indexes). It is possible to obtain three-channel generation under such conditions by increasing the losses for channels 1 and 3. The numerical solution of (1) shows that in this case an increase in the pump power first results in generation in channel 2. The power in this channel increases with an increase in the pump power as long as it is below the generation threshold for channels 1 and 3. A further increase results in an increase in the power of channels 1 and 3, while the channel 2 power drops to zero.

The numerical solution of equation system (1) also shows that at an inter-channel spacing that is larger than 300 GHz when the cross-saturation coefficients are approximately the same (see Fig. 4b), three-channel generation is stable and the powers of all three channels increase steadily as the pump power

increases. This is seen in the experiment at an interchannel spacing of 100 GHz (see Fig. 3).

## CONCLUSIONS

We obtained simultaneous two- or three-wavelength generation in an erbium-fiber laser. The commercial multiplexer that is used to produce the standard DWDM grid in optical fiber communication lines, which was used in this work as a narrow band filter that determined the generation wavelengths, provides a rather simple method for channel wavelength switching. The long-term stability on a several-hour time scale is at least 10%.

In the two-channel generation mode the interchannel frequency spacing can be tuned in the 0.1–4 THz region with a step of 100 GHz. The generation characteristics are described rather well by a simple model in which the interaction between the channels is determined by one independent parameter, viz., the relative cross-saturation coefficient. The experimental and theoretical results are in a good agreement. The cross saturation is maximal in the case of the neighboring channels and decreases as the inter channel frequency spacing increases. An increase in the pump power always results in the stabilization of two-channel generation. In the case of three-channel generation and at a spectral spacing between the channels of 100 GHz, the central channel intensity decreases with the pump power.

## REFERENCES


1. C. Zhang, J. F. Zhao, and C. Y. Miao, Laser Phys. **22**, 1573 (2012).
2. N. G. Basov, M. A. Gubin, V. V. Nikitin, and E. D. Protsenko, Sov. J. Quantum Electron. **14**, 731 (1984). doi 10.1070/QE1984v014n06 ABEH005142
3. O. E. Nanii, Doctoral Dissertation in Mathematics and Physics (Moscow, 1999).
4. O. E. Nanii, E. G. Pavlova, A. A. Susyan, and B. T. Hoan, Laser Phys. **18**, 1238 (2008).
5. F. Aronowitz, in *Laser Applications* (Academic, New York, 1971), pp. 133–200.
6. Ming-Xing Jiao, Yun Liu, and Jun-Hong Xing, J. Phys. Conf. Ser. **48**, 1482 (2007).
7. J. P. Yao, J. Lightwave Technol. **27**, 314 (2009).
8. C. M. Weinert, R. Ludwig, W. Pieper, H. G. Weber, D. Breuer, K. Petermann, and F. Kuuppers, J. Lightwave Technol. **17**, 2276 (1999).
9. M. I. Hayee and A. E. Willner, IEEE Photonics Technol. Lett. **11**, 991 (1999).
10. M. Arikawa, E. T. de Gabory, T. Ito, and K. Fukuchi, in *Proc. Opt. Fiber Commun. Conf., San Francisco, California, USA, 2014.*
11. N. V. Gurkin, V. Mikhailov, O. E. Nanii, A. G. Novikov, V. N. Treshchnikov, and R. R. Ubaydullaev, Laser Phys. Lett. **11**, 095103 (2014).
12. O. V. Yushko, O. E. Nanii, A. A. Redyuk, V. N. Treshchkov, and N. P. Fedoruk, Quantum Electron. **45**, 75 (2015). doi 10.1070/QE2015v045n01ABEH015635
13. A. A. Redyuk, O. E. Nanii, V. N. Treshchikov, V. Mikhailov, and N. P. Fedoruk, Laser Phys. Lett. **12**, 025101 (2015).
14. V. V. Gainov, N. V. Gurkin, S. N. Lukinih, S. G. Akopov, S. Makovejs, S. Y. Ten, O. E. Nanii, and V. N. Treshchikov, Laser Phys. Lett. **10**, 075107 (2013).
15. N. V. Gurkin, Yu. A. Kapin, O. E. Nanii, A. G. Novikov, V. N. Pavlov, S. O. Plaksin, A. Yu. Plotskii, and V. N. Treshchikov, Quant. Electron. **43**, 546 (2013). doi 10.1070/QE2013v043n06ABEH014899
16. V. G. Gudelev, V. V. Mashko, N. K. Nikeenko, G. I. Ryabtsev, A. B. Stalmashonak, and L. L. Teplyashin, Appl. Phys. B: Lasers Opt. **76**, 249 (2003).
17. J. L. Gouet, L. Morvan, M. Alouini, J. Bourderionnet, D. Dolfi, and J. P. Huignard, Opt. Lett. **32**, 1090 (2007).
18. V. G. Voronin, K. P. Dolgaleva, and O. E. Nanii, Quantum Electron **30**, 778 (2000). doi 10.1070/QE2000v030n09ABEH001822
19. V. G. Voronin and O. E. Nanii, Moscow Univ. Phys. Bull. **54** (4), 86 (1999). http://vmu.phys.msu.ru/abstract/1999/4/99-4-64.
20. A. V. Dotsenko, L. S. Kornienko, N. V. Kravtsov, E. G. Lariontsev, O. E. Nanii, and A. N. Shelaevet, Sov. J. Quantum Electron. **16**, 58 (1986). doi 10.1070/QE1986v016n01ABEH005165.
21. O. E. Nanii, Sov. J. Quantum Electron. **22**, 703 (1992). doi 10.1070/QE1992v022n08ABEH003577
22. V. G. Voronin, O. E. Nanii, A. A. Susyan, and V. I. Khlystov, Moscow Univ. Phys. Bull. **65,** 174 (2010). doi 10.3103/S0027134910030045
23. V. G. Voronin, O. E. Nanii, A. A. Sus'yan, and V. I. Khlystov, Quantum Electron. **40**, 111 (2010). doi 10.1070/QE2010v040n02 ABEH014018
24. V. G. Voronin, Ya. V. Sya, O. E. Nanii, and V. I. Khlystov, Quantum Electron. **37**, 339 (2007). doi 10.1070/QE2007v037n04 ABEH013374
25. V. G. Voronin, O. E. Nanii, A. N. Turkin, A. N. Kurkov, S. E. Vasiliev, O. I. Lobadetskii, D. A. Gubankov, and M. N. Nikolaev, Moscow Univ. Phys. Bull. **57** (2), 60 (2002).
26. A. V. Kir'yanov, L. S. Kornienko, N. V. Kravtsov, et al., Moscow Univ. Phys. Bull. **41** (1), 93 (1986).
27. D. V. Zelenin, R. A. Karle, V. N. Petrovskii, and E. D. Protsenko, Quantum Electron. **32**, 5 (2002). doi 10.1070/QE2002v032n01 ABEH002116
28. O. E. Nanii, and A. N. Shelaev, Sov. J. Quantum Electron. **19**, 726 (1989). doi 10.1070/QE1989v019n06ABEH008118

29. J. Yao, J. Yao, Z. Deng, and J. Liu, IEEE Photonics Technol. Lett. **17**, 756 (2005).
30. X. Feng, H.-Y. Tam, C. Lu, et al., IEEE Photonics Technol. **21**, 1314 (2009). doi 10.1109/LPT.2009.2026433
31. N. Park, J. Dawson, and K. J. Vahala, IEEE Photon. Technol. Lett. **4**, 540 (1992).
32. A. Bellemare, M. Karasek, M. Rochette, and M. Têtu, J. Lightwave Technol. **18**, 825 (2000).
33. O. E. Nanii, Quantum Electron. **26**, 15 (1996). doi 10.1070/QE1996v026n01 ABEH000575
34. M. Bolshtyansky, J. Lightwave Technol. **21**, 1032 (2003).
35. Z. L. Hu, P. Xu, and N. Jiang, Laser Phys. **2**, 1590 (2012).
36. *ITU-T G.694.1. Spectral grids for WDM applications: DWDM frequency grid*. https://www.itu.int/rec/T-REC-G.694.1-200206-S/en.

*Translated by V. Alekseev*